

OPEN

Retina Publish Ahead of Print

DOI: 10.1097/IAE.0000000000004506

Incidence, Characteristics, and Outcomes of Macular Neovascularization in Extensive Macular Atrophy with Pseudodrusen-like Appearance.

Andrea Trinco MD¹, Alessio Antropoli MD², Lorenzo Bianco MD², Chiara Zaffalon MD³, Matteo Airaldi MD FEBO^{4,5}, Alessandro Lanzani MD³, Mariano Cozzi MSc PhD¹, Alessandro Invernizzi MD^{1,6}, Alessandro Arrigo MD PhD², Andrea Saladino MD², Francesco Bandello MD², Francesca Bosello MD³, Stefano Casati MD³, Anna Paola Salvetti MD¹, Maurizio Battaglia Parodi MD², Giovanni Staurenghi MD FARVO^{1,*†} and Francesco Romano MD FEBO^{1,7,*}

This is an open-access article distributed under the terms of the Creative Commons Attribution-Non Commercial-No Derivatives License 4.0 (CCBY-NC-ND), where it is permissible to download and share the work provided it is properly cited. The work cannot be changed in any way or used commercially without permission from the journal.

AFFILIATIONS

¹ Eye Clinic, Department of Biomedical and Clinical Sciences, Ospedale Luigi Sacco, University of Milan, Milan, Italy

² Department of Ophthalmology, IRCCS San Raffaele Scientific Institute, Milan, Italy
University Vita-Salute San Raffaele, Milan, Italy

³ Ophthalmic Unit, Department of Neurosciences, Biomedicine and Movement Sciences, University of Verona, Verona, Italy

⁴ Department of Medical and Surgical Specialties, Radiological Sciences, and Public Health, University of Brescia, Brescia, Italy

⁵ St Paul's Eye Unit, Royal Liverpool and Broadgreen University Hospitals, University of Liverpool, Liverpool, UK

⁶ Save Sight Institute, University of Sydney, Sydney, NSW, Australia

⁷ Harvard Retinal Imaging Lab, Retina Service, Department of Ophthalmology, Massachusetts Eye and Ear, Harvard Medical School, Boston, MA, USA

* Co-senior last authors

† Corresponding author

CORRESPONDING AUTHOR

Prof. Giovanni Staurenghi, MD FARVO

Eye Clinic, Department of Biomedical and Clinical Sciences, Luigi Sacco Hospital, University of Milan

Via G.B. Grassi, 74 – 20157, Milan (Italy)

E-mail address: giovanni.staurenghi@unimi.it | Tel: +39 02 39042901 | Fax: +39 02 50319843

Word Count: 2999.

Short Title: Macular Neovascularization in EMAP.

Financial Support: none relevant to this research.

Conflict of Interest: no conflicting relationship relevant to this research.

Financial Disclosures: AT, AA, LB, CZ, MA, AL, AA, AS, Francesca Bosello, SC, APS, and MBP have no relevant disclosures. MC is recipient from Bayer HealthCare, Nidek, Novartis, Heidelberg Engineering, and Zeiss. AI is consultant for Bayer, Novartis, and Roche. Francesco Bandello is consultant for Allergan Inc (Irvine, California, USA), Bayer Shering-Pharma (Berlin, Germany), Hoffmann-La-Roche (Basel, Switzerland), Novartis (Basel, Switzerland), Sanofi-Aventis (Paris, France), Thrombogenics (Heverlee, Belgium), Zeiss (Dublin, USA), Boehringer-Ingelheim, Fidia Sooft, Ntc Pharma, Sifi. GS is consultant for Heidelberg Engineering, Optos, OptoVue, CenterVue, Allergan, Bayer, Genetech, Novartis, Quantel Medical, Carl Zeiss Meditec, Boehringer, Topcon, Roche. FR is co-inventor on a patent through Massachusetts Eye and Ear (U.S. 63/381,925).

Keywords: EMAP; extensive macular atrophy with pseudodrusen-like appearance; macular neovascularization; MNV; incidence; risk factors; outcomes; CNV.

Summary Statement: We estimated a cumulative incidence of MNV in EMAP of 15.2% at 4 years (4.2% excluding left-censored data), most being type 2 lesions and located subfoveally. While BCVA changes were comparable, MNV eyes showed faster RPE atrophy progression, suggesting a more aggressive phenotype or increased fibro-atrophic changes.

ABSTRACT

Purpose: To report the incidence, features, and clinical outcomes of macular neovascularization (MNV) in a large Italian cohort of patients with extensive macular atrophy with pseudodrusen-like appearance (EMAP).

Methods: Retrospective, longitudinal study including 79 EMAP patients (158 eyes) with ≥ 6 months of follow-up at three retina clinics. Medical records and imaging were reviewed for demographic and clinical data, including age, best-corrected visual acuity (BCVA), MNV features, and retinal pigment epithelium (RPE) atrophy size, measured by short-wavelength autofluorescence and refined with near-infrared and OCT imaging. Main outcomes included cumulative MNV incidence, MNV risk factors, and BCVA and RPE atrophy changes in eyes with and without MNV.

Results: Over a mean follow-up of 40.4 months, MNV developed in 14 eyes (10 patients), with a 4-year cumulative incidence of 15.2%. Most MNVs were type 2 (86%) and subfoveal (64%). Cox regression identified younger age, fellow eye involvement, smaller RPE atrophy size, and greater central subfield thickness (all $p < 0.01$) as significant risk factors for MNV. While eyes with MNV had lower baseline BCVA (58.4 vs. 71.4 letters, approximately 20/63 vs. 20/40 Snellen; $p = 0.005$), BCVA decline over time was similar between the two groups (-3.9 vs. -4.1 letters/year, $p = 0.69$). However, RPE atrophy progressed faster in MNV eyes (3.4 vs. 2.8 mm²/year, $p = 0.02$).

Conclusions: In this EMAP cohort, MNV had a cumulative incidence of 15.2% at 4 years. Although BCVA outcomes were comparable, MNV was associated with faster atrophy progression, potentially due to a more aggressive disease phenotype or fibro-atrophic changes.

INTRODUCTION

Extensive macular atrophy with pseudodrusen-like appearance (EMAP) is a severe bilateral retinal degenerative disorder first described in France by Hamel *et al.*¹ EMAP predominantly affects middle-aged women, though onset can vary, and typically leads to legal blindness within five years.^{1,2} While its precise etiology remains unclear, the EMAP Case-Control National Clinical Trial identified links with chronic low-dose organophosphates exposure and nonspecific complement system activation.^{3,4}

EMAP diagnosis is primarily clinical, based on a triad of vertically-oriented macular atrophy, diffuse pseudodrusen-like deposits, and peripheral paving stones.^{1,5,6} Advances in retinal imaging have identified additional key features, including the separation between the retinal pigment epithelium (RPE) and Bruch's membrane (BrM) preceding atrophy, BrM ruptures, and an oval area of relative photoreceptor-RPE sparing, located temporal to the macula.^{5,7-10}

Romano *et al.* developed the first EMAP classification based on longitudinal observations over three years.^{5,11} Stage 1 is characterized by RPE-BrM separation with few or no confluent areas of atrophy and preserved visual acuity. Stage 2 involves more extensive confluent areas of atrophy without foveal involvement, while stage 3 presents with significant visual loss due to foveal involvement – either from expansion of macular atrophy or development of subfoveal non-neovascular fibrosis.

Recently, macular neovascularization (MNV) has been reported as a complication of EMAP, contributing to additional visual loss.^{5,10,12} Information on this rare complication is limited to few reports.¹³⁻¹⁵ Romano *et al* included MNV as a '+' feature in their classification, indicating its possible occurrence at any stage. However, longitudinal data on MNV characteristics and their

outcomes remain scarce. This study aims to report the incidence, clinical characteristics, and long-term outcomes of MNV in a large cohort of EMAP patients from three Italian referral clinics.

METHODS

This retrospective, longitudinal study included data from three Italian referral centers for retinal disorders: Ospedale Luigi Sacco (Milan), Ospedale San Raffaele (Milan), and Ospedale Borgo Roma (Verona). The research adhered to the Declaration of Helsinki. Institutional review board (IRB) approval was obtained from each center, and all participants provided written informed consent.

We reviewed electronic medical records and imaging studies of EMAP patients followed at these clinics between January 2009 and February 2024. Inclusion criteria were: (1) diagnosis of EMAP based on the classic clinical triad,¹ (2) age <55 years at diagnosis or symptoms onset, (3) at least two clinical examinations with retinal imaging over a follow-up of ≥ 6 months, and (4) negative genetic test for inherited phenocopies of EMAP using next-generation sequencing (Illumina MiSeq; Illumina, San Diego, CA), including screening for late-onset retinal degeneration (L-ORD; C1QTNF5, OMIM #605670), Sorsby fundus dystrophy (SFD; TIMP3, OMIM #136900), and pseudoxanthoma elasticum (PXE; ABCC6, OMIM #264800).^{2,16} Exclusion criteria included: (1) other ocular or systemic conditions affecting the analysis, (2) refractive errors exceeding |6| diopters, (3) media opacities impairing image quality, and (4) history of intraocular inflammation or ocular surgery other than cataract extraction and intravitreal anti-VEGF injections.

Retinal imaging required for eligibility included fundus photographs (Sacco: EIDON, CenterVue from 2016; previously FF 450plus, Carl Zeiss; San Raffaele & Borgo Roma: Optos California, Optos plc. from 2015; previously TRC-50DX, Topcon), 30°x30° short-wavelength autofluorescence (SW-AF) and macular spectral-domain optical coherence tomography (SD-OCT; at least 20°x20°, centered on the fovea) using the Spectralis HRA+OCT system (Heidelberg Engineering GmbH, Heidelberg, Germany). Given the retrospective design, follow-up and

treatment strategies were not standardized across centers. However, common protocols were: (a) follow-up every 6-12 months for patients without MNV, (b) anti-VEGF treatment for active MNV, and (c) monthly monitoring for active MNV cases, with extended intervals (up to 4 months) once inactivity was achieved.

Study Protocol and Data Collection

Baseline and follow-up data collected included demographic and clinical information: age, sex, smoking status, lens status, best-corrected visual acuity (BCVA, converted to early treatment for diabetic retinopathy study [ETDRS] letters), presence of MNV, anti-VEGF agent used (bevacizumab, ranibizumab, aflibercept), and lesion activity (percentage of visits with active MNV). The frequency of anti-VEGF injections and lesion activity were reported annually, as previously described.¹⁷

MNV diagnosis required identification of a neovascular network on indocyanine green angiography (ICGA) or, if contraindicated, OCT angiography, along with leakage on fluorescein angiography (FA).¹⁸ Treatment was initiated with either a single intravitreal anti-VEGF injection or a loading dose of three monthly injections, as determined by the treating physician, followed by a *pro re nata* (PRN) regimen. Re-treatment criteria included: (1) persistent or recurrent intra-/sub-retinal exudation, (2) significant growth or undefined neovascular membrane margins on SD-OCT, (3) hemorrhages on fundus photography, or (4) leakage on FA.¹⁹

Imaging Analysis

Imaging studies from all available visits were independently graded by two masked retina specialists (F.R. and M.B.P.) using Heidelberg Eye Explorer software (HEYEX; version 1.10.4.0, Heidelberg Engineering GmbH, Germany). Any qualitative discrepancies and quantitative measurements differing by >10% were resolved by a third senior grader (G.S.).

30°x30° SW-AF images were analyzed to measure the size of RPE atrophy and assess the autofluorescence signal at the atrophic borders (iso- or hyper-autofluorescent).^{2,20} Specifically, RPE atrophy areas, which appeared hypo-autofluorescent, were measured with the semi-automated Heidelberg RegionFinder tool (version 2.6.4) and manually adjusted using co-registered near-infrared (bright hyperreflectivity) and SD-OCT (outer retinal and RPE loss) scans to exclude other hypo-autofluorescent lesions (e.g., macular pigments, hemorrhages, and RPE tears).^{21,22,2}

The following SD-OCT biomarkers were assessed: (1) presence of any vitreomacular interface disorder (VMID),²³ (2) central subfield thickness (CST),²⁴ defined as the distance from the internal limiting membrane to BrM within the central 1 mm circle, (3) outer retinal tubulations (ORTs),²⁵ and (4) subfoveal choroidal thickness (SCT), measured from the outer RPE line to the sclero-choroidal interface.²⁶ Non-neovascular fibrosis (stage 3b) was identified on fundus photographs as a well-demarcated mound of yellowish-white tissue, without exudative signs on SD-OCT or a neovascular network on OCT angiography.^{5,27}

For eyes with MNV, baseline images were reviewed to determine the type and location of neovascularization, based on the CONAN (type 1, 2, 3, or polypoidal choroidal vasculopathy) and CATT study group criteria.^{18,28} Specifically, MNV location was categorized as subfoveal (involving the foveal center), juxtafoveal (1-200 µm from the foveal center), or extrafoveal (>200 µm) using ICGA images, obtained 1-to-10 minutes post-injection, and overlaid on near-infrared and SD-OCT scans.¹⁷

Statistical analysis

All analyses were conducted using Stata/MP 18 (StataCorp; College Station, TX, USA) and R Studio Version 2023.12.0+369 (RStudio, PBC; Boston, MA). Significance was considered at $\alpha < 0.05$ for two-sided tests. Descriptive statistics included mean (standard deviation, SD), median (interquartile range, IQR), or frequencies (%), with variable distributions assessed via Shapiro-Wilk

test. Inter-grader agreement was evaluated using Cohen's kappa for categorical measurements and two-way mixed-effects intraclass correlation coefficients (ICCs) for continuous data.

MNV incidence was calculated per 100 person-years, and cumulative incidence was presented using Kaplan-Meier estimates (expressed as %), both for the whole cohort and after excluding left-censored data (MNV at baseline). Mixed-effects Cox regression determined the risk factors for MNV development, reported as hazard ratios (HR). Time-varying variables included age, smoking status, fellow eye involvement, atrophy borders, RPE atrophy size, VMID, CST, SCT, and ORT. Only variables significant in univariable analysis were considered in multivariable models. Linear mixed-effects models assessed the effects of MNV, time, and their interaction term on BCVA and RPE atrophy size, adjusted for baseline values and age. Random intercepts accounted for data hierarchy (eyes nested within patients). Scaling was applied to age (per 0.1), CST (per 0.01), and square-rooted RPE atrophy size to enhance model stability and account for baseline lesion size. Results are reported as mean estimates with 95% confidence intervals (95% CI).

RESULTS

Our study included 158 eyes from 79 EMAP patients, predominantly female (52, 65.8%), with a median age of 57.3 years [IQR: 53.8-60.4] at baseline. Of the 176 eyes initially considered (88 patients), 18 eyes from 9 patients were excluded due to insufficient follow-up (8 eyes), glaucoma (4 eyes), high refractive errors (4 eyes), and prior subthreshold laser treatment (2 eyes).

The mean baseline BCVA was 70.7 [SD: 21.0] ETDRS letters (approximately 20/40 Snellen), with a median RPE atrophy size of 8.2 mm² [IQR: 2.2-18.0]. Table 1 summarizes the demographic and clinical characteristics. Inter-grader agreement was substantial-to-good for all variables (Supplemental Digital Content 1).

Characteristics of the MNV

MNV was identified in 14 eyes (8.9%) of 10 patients, with bilateral involvement in 4 patients (40%). MNV was present at baseline in 8 eyes (57.1%). MNV onset was associated with visual symptoms in 11 cases (78.6%). Most lesions were type 2 (12 eyes, 85.7%) and primarily subfoveal (9 eyes, 64.3%) (Figure 1). MNVs were active in 41.7% [SD: 23.9] of visits during the first year and responded well to anti-VEGF treatment, with a median of 2 [IQR: 1–3.8] injections needed in the first year and reactivations in 4 eyes (28.6%). Notably, 3 eyes (21.4%) experienced a significant BCVA decline attributable to fibrovascular scarring from MNV, while most cases had stable or improved vision following treatment. One eye (7.1%) developed an RPE tear following anti-VEGF treatment. Median RPE atrophy size at MNV onset was 9.1 mm² [IQR: 6.2-22.1], with a bimodal distribution (peaks at 3.1-6.0 mm² and 21.1-24.0 mm²; Figure 2). Specifically, MNV cases were classified as stage 1 (5 eyes, 35.7%), stage 2 (6 eyes, 42.9%), and stage 3 (3 eyes, 21.4%) (Table 2).

Incidence and Factors Associated with MNV

Over a mean follow-up of 40.4 months, MNV developed in 14 eyes, yielding a cumulative incidence of 6.1% [4.1-8.0] at 1 year and 15.2% [11.6-18.7] at 4 years. Excluding left-censored data, the cumulative incidence was 0.9% [0.0-2.7] at 1 year and 4.2% [0.0-8.9] at 4 years. The median incidence rate was 2.3 [1.0-3.6] events per 100 person-years (1.2 [0.2-2.2] after excluding left-censored data). The Kaplan-Meier curve of MNV incidence is shown in Figure 3A.

Univariable Cox regression revealed that younger age (per 0.1; HR=0.001, p<0.001), fellow eye involvement (HR=2.1, p<0.001), smaller RPE atrophy size (HR=0.51, p<0.001), greater CST (HR=2.1, p=0.002), and greater SCT (per 0.01; HR=19.1, p<0.001) were associated with a higher MNV risk. Multivariable Cox regression confirmed associations with younger age (HR=0.03, p<0.001), fellow eye involvement (HR=18.4, p=0.01), smaller RPE atrophy size (HR=0.63, p=0.001), and greater CST (per 0.01; HR=2.2, p=0.002) (Figure 3B and Table 3).

Impact of MNV on BCVA and RPE Atrophy

Eyes with MNV had lower baseline BCVA compared to those without MNV (58.4 vs. 71.4 ETDRS letters, approximately 20/63 vs. 20/40 Snellen; $\beta = -12.9$, $p = 0.005$). However, after adjusting for age and baseline BCVA, the rate of BCVA decline was similar between groups (-3.9 vs. -4.1 ETDRS letters/year; $\beta = 0.24$, $p = 0.69$).

At baseline, eyes with MNV had a moderately smaller, though not significant, RPE atrophy size (5.6 vs. 11.9 mm²; $\beta = -0.25$, $p = 0.27$). After adjusting for age and baseline RPE atrophy size, eyes with MNV showed a faster rate of RPE atrophy growth compared to those without MNV (3.4 vs. 2.8 mm²/year; $\beta = 0.05$, $p = 0.02$). Changes in BCVA and RPE atrophy size over time are shown in Figure 4. Figure 5 illustrates RPE atrophy measurements over time in an eye with MNV.

No significant associations were found between MNV lesion activity and the rates of RPE atrophy growth ($\beta = 0.002$, $p = 0.88$) or BCVA loss ($\beta = 0.14$, $p = 0.12$).

DISCUSSION

This study retrospectively analyzed the incidence, clinical features, and risk factors for MNV in a large Italian cohort of 79 EMAP patients. Most MNV cases were type 2, predominantly subfoveal, and demonstrated a favorable anatomical response to anti-VEGF treatment. We also evaluated the impact of MNV on visual outcomes and RPE atrophy progression. While MNV had limited impact on BCVA after treatment, it was associated with a significantly faster rate of RPE atrophy growth in affected eyes.

EMAP is an increasingly recognized retinal degeneration leading to legal blindness within five years from onset.^{1,2,10,12} Visual loss is generally due to foveal RPE atrophy or subfoveal non-neovascular fibrosis,⁵ though MNV can occasionally worsen visual outcomes. Prior studies on MNV in EMAP are limited and mostly consist of isolated case reports.¹²⁻¹⁵ Kamamy-Levy *et al*¹⁵ reported choroidal neovascularization in approximately 10% of their cohort (4 eyes from 3 patients), with good anatomical but limited functional response to anti-VEGF or laser treatment. More recently, Antropoli *et al*.¹² identified choroidal neovascularization in 19 cases (14.7%) in a

large French cohort, though extra-macular cases were included and clinical outcomes were not assessed.

In our study, MNV developed in 14 eyes over a mean follow-up of ~40 months, with a cumulative incidence of 6.1% at 1 year and 15.2% at 4 years for this complication (0.9% and 4.2% after excluding baseline MNV). These rates align with those reported by Kamamy-Levy and Antropoli,^{12,15} and with the prevalence of exudative MNV in geographic atrophy (GA) from AMD.^{29,30} Although MNV incidence in L-ORD –a phenocopy of EMAP– remains uncertain,³¹ the rates in our cohort are notably lower than in other phenocopies like PXE (42-86%) and SFD (60-80%).^{32,33} The high incidence in PXE may reflect BrM degradation and disrupted RPE-choriocapillaris communication, leading to VEGF upregulation,^{34,35} while differences with SFD suggest distinct angiogenic mechanisms in EMAP despite imaging similarities.

Most MNV cases in our study were type 2 (85.7%) and subfoveal (64.7%) lesions, consistent with patterns seen in GA and inherited EMAP phenocopies.^{15,29} This may reflect the significant EMAP-associated RPE alterations, which compromise the barrier function and promote subretinal invasion. Interestingly, unlike AMD,³⁶ we found no type 3 MNV cases, despite the presence of pseudodrusen-like deposits. Table 4 summarizes the clinical and MNV characteristics of EMAP and its phenocopies. Although treatment protocols varied, all MNV cases responded well to anti-VEGF injections on a PRN basis. The median number of injections in the first year was two, with fewer reactivations over time – suggesting PRN may be an effective approach for MNV in EMAP.

Furthermore, Cox regression analysis identified several factors associated with MNV development in EMAP. The increased risk with fellow eye involvement may indicate strong inter-eye dependence, similar to AMD.³⁷ However, the associations with younger age, smaller RPE atrophy size, and greater CST suggest that neovascular complications are more likely in the earlier stages of EMAP. This may represent a para-physiological response to support hypoxic photoreceptors and locally inhibit RPE atrophy progression, as proposed in AMD.³⁸ We also observed a bimodal distribution of MNV occurrence by RPE atrophy size, with peaks around 3.1-

6.0 mm² (stage 1) and 21.1–24.0 mm² (transition to stage 3). The first peak may reflect increased VEGF production from viable RPE in response to the diffuse RPE-BrM separation acting as a barrier to photoreceptor nutrition.^{7,9} The second peak could indicate a late attempt to protect the fovea or result from BrM ruptures, which have been reported in 25% of late-stage EMAP cases.¹² Based on these findings, and the asymptomatic nature of MNV in some cases, we recommend closer monitoring during stages 1 and 2, particularly for patients with fellow eye involvement.

Lastly, the recent FDA approval of anti-complement treatments for GA has sparked interest in their potential application to other forms of macular atrophy.³⁹ This is especially relevant given EMAP's resemblance to the diffuse-trickling phenotype of GA and the altered complement levels detected in the initial French cohort.^{4,6} However, since anti-complement therapy in AMD has been associated with higher MNV rates,^{40,41} understanding the clinical impact of MNV in EMAP—beyond its incidence—becomes essential. While MNV was associated with worse BCVA at presentation (59 vs. 71 ETDRS letters, approximately 20/63 vs. 20/40 Snellen), we found no significant difference in BCVA decline over time between EMAP eyes with and without MNV. In contrast, RPE atrophy progression was faster in MNV eyes (3.4 mm² vs. 2.8 mm²/year), even after adjusting for baseline size, diverging from previous clinical and histological findings in AMD.^{21,30,42} Potential explanations for accelerated atrophy in MNV eyes include: (1) MNV-related fibro-atrophic changes, particularly due to the high prevalence of type 2 lesions; (2) possible side effects of physiological VEGF levels suppression, though patients received few injections and lesion activity was not correlated with atrophy growth; and (3) a more aggressive EMAP phenotype characterized by MNV and rapid atrophy progression. Studying untreated EMAP cohorts may help clarify this aspect. Yet, we cannot rule out that current models using square-root transformation and adjustment for baseline size may not fully capture the exponential growth of macular atrophy in EMAP, suggesting a need for alternative regression models for atrophy assessment.

It is important to acknowledge some limitations, particularly the retrospective design, which prevented standardized follow-up and treatment protocols across centers. While the number of

MNV cases was relatively small (14), MNV is a rare complication of EMAP, and our cohort remains one of the largest with longitudinal follow-up in the literature. Additionally, functional tests such as microperimetry may correlate more closely with EMAP stages than BCVA alone.¹¹ Future studies incorporating functional assessments beyond BCVA may offer a more nuanced understanding of MNV's impact on visual function. We also did not assess extra-macular neovascularization due to the lack of standardized widefield imaging, and non-exudative type 1 MNV may have been missed in the absence of routine longitudinal OCTA assessments. Moreover, while BrM ruptures have recently emerged as a relevant biomarker in advanced EMAP, its low prevalence in our relatively younger cohort precluded its inclusion in the statistical analysis. We look forward to exploring the relationship between BrM ruptures and MNV in future prospective studies. Lastly, measuring RPE atrophy using SW-AF can be challenging in eyes with MNV.^{22,43} To minimize this, we employed a validated method incorporating near-infrared imaging and structural OCT,²² which resulted in excellent intergrader agreement.

To conclude, we reported a 4-year cumulative incidence of 15.2% for MNV in a large Italian cohort of EMAP patients, identifying younger age and smaller RPE atrophy size as significant risk factors. The high prevalence of type 2 lesions and the bimodal distribution of RPE atrophy size at MNV onset suggest two possible pathways in MNV pathogenesis: (1) early-stage involvement of a dysfunctional yet viable RPE layer, and (2) BrM ruptures promoting neovascularization in more advanced stages. Clinically, while anti-VEGF treatment led to prompt BCVA improvement, RPE atrophy expanded more rapidly in MNV eyes, potentially due to fibrosis-related atrophic changes or a more aggressive disease phenotype. These findings provide critical insights into EMAP's natural history and may guide future targeted therapies aimed at slowing macular atrophy growth.

SDC_1--<http://links.lww.com/IAE/C568>

REFERENCES.

1. Hamel CP, Meunier I, Arndt C, et al. Extensive macular atrophy with pseudodrusen-like appearance: a new clinical entity. *Am J Ophthalmol.* 2009;147(4):609-620. doi:10.1016/j.ajo.2008.10.022
2. Romano F, Airaldi M, Cozzi M, et al. Progression of Atrophy and Visual Outcomes in Extensive Macular Atrophy with Pseudodrusen-like Appearance. *Ophthalmol Sci.* 2021;1(1):100016. doi:10.1016/j.xops.2021.100016
3. Douillard A, Picot MC, Delcourt C, et al. Clinical Characteristics and Risk Factors of Extensive Macular Atrophy with Pseudodrusen: The EMAP Case-Control National Clinical Trial. *Ophthalmology.* 2016;123(9):1865-1873. doi:10.1016/j.ophtha.2016.05.018
4. Douillard A, Picot MC, Delcourt C, et al. Dietary, environmental, and genetic risk factors of Extensive Macular Atrophy with Pseudodrusen, a severe bilateral macular atrophy of middle-aged patients. *Sci Rep.* 2018;8(1):6840. doi:10.1038/s41598-018-25003-9
5. Romano F, Cozzi M, Monteduro D, et al. NATURAL COURSE AND CLASSIFICATION OF EXTENSIVE MACULAR ATROPHY WITH PSEUDODRUSEN-LIKE APPEARANCE. *Retina.* 2023;43(3):402-411. doi:10.1097/IAE.0000000000003683
6. Antropoli A, Arrigo A, Bianco L, et al. Quantitative multimodal imaging of extensive macular atrophy with pseudodrusen and geographic atrophy with diffuse trickling pattern. *Sci Rep.* 2023;13(1):1822. doi:10.1038/s41598-023-28906-4
7. Romano F, Cozzi M, Casati S, et al. Unveiling the Hidden: Early Manifestations of Extensive Macular Atrophy with Pseudodrusen-like appearance. *Retin Cases Brief Rep.* Published online November 1, 2023. doi:10.1097/ICB.0000000000001513
8. Bianco L, Antropoli A, Arrigo A, et al. Fundus autofluorescence in Extensive Macular Atrophy with Pseudodrusen (EMAP) and Diffuse Trickling Geographic Atrophy (DTGA). *Retina.* Published online January 2, 2023. doi:10.1097/IAE.0000000000003733

9. Fragiotta S, Parravano M, Sacconi R, et al. A COMMON FINDING IN FOVEAL-SPARING EXTENSIVE MACULAR ATROPHY WITH PSEUDODRUSEN IMPLICATES BASAL LAMINAR DEPOSITS. *Retina*. 2022;42(7):1319-1329. doi:10.1097/IAE.0000000000003463
10. Antropoli A, Bianco L, Romano F, et al. Extensive macular atrophy with pseudodrusen-like appearance (EMAP) clinical characteristics, diagnostic criteria, and insights from allied inherited retinal diseases and age-related macular degeneration. *Prog Retin Eye Res*. 2025;104:101320. doi: 10.1016/j.preteyeres.2024.101320.
11. Romano F, Boon CJF, Invernizzi A, et al. CORRELATION BETWEEN MICROPERIMETRY AND IMAGING IN EXTENSIVE MACULAR ATROPHY WITH PSEUDODRUSEN-LIKE APPEARANCE. *Retina*. 2024;44(2):246-254. doi:10.1097/IAE.0000000000003951
12. Antropoli A, Bianco L, Condroyer C, et al. Extensive Macular Atrophy with Pseudodrusen-like appearance: Progression Kinetics and Late-Stage Findings. *Ophthalmology*. Published online April 6, 2024:S0161-6420(24)00209-4. doi:10.1016/j.opthta.2024.04.001
13. Parodi MB, Querques G. Choroidal neovascularization associated with extensive macular atrophy and pseudodrusen. *Optom Vis Sci*. 2015;92(4 Suppl 1):S51-54. doi:10.1097/OPX.0000000000000532
14. Romano D, Colombo L, Maltese P, et al. BRUCH MEMBRANE RUPTURE AND CHOROIDAL NEOVASCULARIZATION COMPLICATING EXTENSIVE MACULAR ATROPHY WITH PSEUDODRUSEN-LIKE APPEARANCE: A CASE REPORT. *Retin Cases Brief Rep*. 2023;17(5):557-561. doi:10.1097/ICB.0000000000001236
15. Kamami-Levy C, Querques G, Rostaqui O, et al. Choroidal neovascularization associated with extensive macular atrophy with pseudodrusen-like appearance. *J Fr Ophtalmol*. 2014;37(10):780-786. doi:10.1016/j.jfo.2014.06.003
16. Rajabian F, Arrigo A, Bordato A, et al. Optical Coherence Tomography Angiography in Extensive Macular Atrophy with Pseudodrusen-Like Appearance. *Transl Vis Sci Technol*. 2020;9(3):2. doi:10.1167/tvst.9.3.2

17. Romano F, Cozzi E, Airaldi M, et al. Ten-Year Incidence of Fibrosis and Risk Factors for Its Development in Neovascular Age-Related Macular Degeneration. *Am J Ophthalmol.* 2023;252:170-181. doi:10.1016/j.ajo.2023.03.033
18. Told R, Sacu S, Hecht A, et al. Comparison of SD-Optical Coherence Tomography Angiography and Indocyanine Green Angiography in Type 1 and 2 Neovascular Age-related Macular Degeneration. *Invest Ophthalmol Vis Sci.* 2018;59(6):2393-2400. doi:10.1167/iovs.17-22902
19. Spaide RF, Jaffe GJ, Sarraf D, et al. Consensus Nomenclature for Reporting Neovascular Age-Related Macular Degeneration Data: Consensus on Neovascular Age-Related Macular Degeneration Nomenclature Study Group. *Ophthalmology.* 2020;127(5):616-636. doi:10.1016/j.ophtha.2019.11.004
20. Fleckenstein M, Mitchell P, Freund KB, et al. The Progression of Geographic Atrophy Secondary to Age-Related Macular Degeneration. *Ophthalmology.* 2018;125(3):369-390. doi:10.1016/j.ophtha.2017.08.038
21. Sadda SR, Tuomi LL, Ding B, et al. Macular Atrophy in the HARBOR Study for Neovascular Age-Related Macular Degeneration. *Ophthalmology.* 2018;125(6):878-886. doi:10.1016/j.ophtha.2017.12.026
22. Spooner KL, Fraser-Bell S, Cozzi M, et al. Macular Atrophy Incidence and Progression in Eyes with Neovascular Age-Related Macular Degeneration Treated with Vascular Endothelial Growth Factor Inhibitors Using a Treat-and-Extend or a Pro Re Nata Regimen: Four-Year Results of the MANEX Study. *Ophthalmology.* 2020;127(12):1663-1673. doi:10.1016/j.ophtha.2020.06.019
23. Duker JS, Kaiser PK, Binder S, et al. The International Vitreomacular Traction Study Group classification of vitreomacular adhesion, traction, and macular hole. *Ophthalmology.* 2013;120(12):2611-2619. doi:10.1016/j.ophtha.2013.07.042

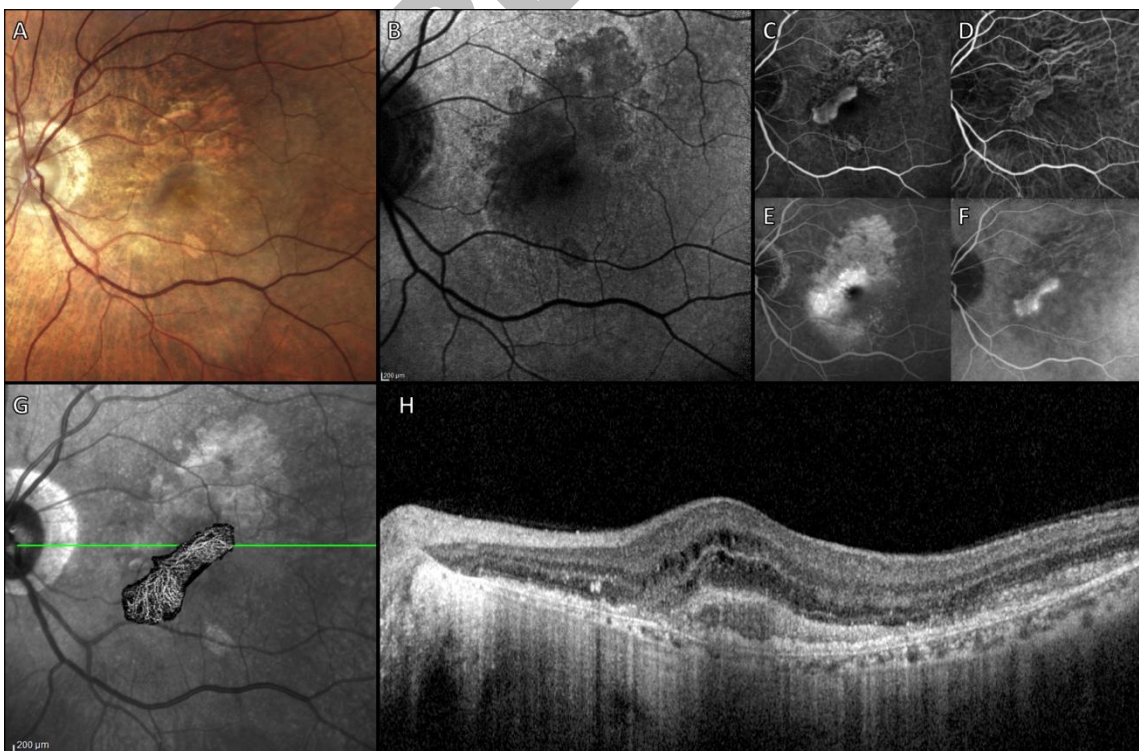
24. Sun JK, Josic K, Melia M, et al. Conversion of Central Subfield Thickness Measurements of Diabetic Macular Edema Across Cirrus and Spectralis Optical Coherence Tomography Instruments. *Transl Vis Sci Technol.* 2021;10(14):34. doi:10.1167/tvst.10.14.34
25. Zweifel SA, Engelbert M, Laud K, et al. Outer retinal tubulation: a novel optical coherence tomography finding. *Arch Ophthalmol.* 2009;127(12):1596-1602. doi:10.1001/archophthalmol.2009.326
26. Rahman W, Chen FK, Yeoh J, et al. Repeatability of manual subfoveal choroidal thickness measurements in healthy subjects using the technique of enhanced depth imaging optical coherence tomography. *Invest Ophthalmol Vis Sci.* 2011;52(5):2267-2271. doi:10.1167/iovs.10-6024
27. Toth LA, Stevenson M, Chakravarthy U. ANTI-VASCULAR ENDOTHELIAL GROWTH FACTOR THERAPY FOR NEOVASCULAR AGE-RELATED MACULAR DEGENERATION: Outcomes in Eyes With Poor Initial Vision. *Retina.* 2015;35(10):1957-1963. doi:10.1097/IAE.0000000000000583
28. Laser photocoagulation of subfoveal neovascular lesions of age-related macular degeneration. Updated findings from two clinical trials. Macular Photocoagulation Study Group. *Arch Ophthalmol.* 1993;111(9):1200-1209. doi:10.1001/archopht.1993.01090090052019
29. Sacconi R, Brambati M, Miere A, et al. Characterisation of macular neovascularisation in geographic atrophy. *Br J Ophthalmol.* 2022;106(9):1282-1287. doi:10.1136/bjophthalmol-2021-318820
30. Airaldi M, Corvi F, Cozzi M, et al. Differences in Long-Term Progression of Atrophy between Neovascular and Nonneovascular Age-Related Macular Degeneration. *Ophthalmol Retina.* 2022;6(10):914-921. doi:10.1016/j.oret.2022.04.012
31. Heath Jeffery RC, Chen FK. Macular neovascularization in inherited retinal diseases: A review. *Surv Ophthalmol.* 2024;69(1):1-23. doi:10.1016/j.survophthal.2023.07.007

32. Risseeuw S, Ossewaarde-van Norel J, Klaver CCW, et al. VISUAL ACUITY IN PSEUDOXANTHOMA ELASTICUM. *Retina*. 2019;39(8):1580-1587. doi:10.1097/IAE.0000000000002173
33. Sivaprasad S, Webster AR, Egan CA, et al. Clinical course and treatment outcomes of Sorsby fundus dystrophy. *Am J Ophthalmol*. 2008;146(2):228-234. doi:10.1016/j.ajo.2008.03.024
34. Keir LS, Firth R, Aponik L, et al. VEGF regulates local inhibitory complement proteins in the eye and kidney. *J Clin Invest*. 2017;127(1):199-214. doi:10.1172/JCI86418
35. Blaauwgeers HG, Holtkamp GM, Rutten H, et al. Polarized vascular endothelial growth factor secretion by human retinal pigment epithelium and localization of vascular endothelial growth factor receptors on the inner choriocapillaris. Evidence for a trophic paracrine relation. *Am J Pathol*. 1999;155(2):421-428. doi:10.1016/S0002-9440(10)65138-3
36. Spaide RF, Ooto S, Curcio CA. Subretinal drusenoid deposits AKA pseudodrusen. *Surv Ophthalmol*. 2018;63(6):782-815. doi:10.1016/j.survophthal.2018.05.005
37. Giuffrida FP, Nassisi M, de Sanctis L, et al. Ten-Year Follow-Up of Fellow Eyes in Patients with Unilateral Naïve Exudative AMD. *Retina*. Published online August 14, 2024. doi:10.1097/IAE.0000000000004251
38. Chen L, Messinger JD, Sloan KR, et al. Nonexudative Macular Neovascularization Supporting Outer Retina in Age-Related Macular Degeneration: A Clinicopathologic Correlation. *Ophthalmology*. 2020;127(7):931-947. doi:10.1016/j.optha.2020.01.040
39. Chew EY. Complement inhibitors for the treatment of geographic atrophy. *Lancet*. 2023;402(10411):1396-1398. doi:10.1016/S0140-6736(23)01844-5
40. Heier JS, Lad EM, Holz FG, et al. Pegcetacoplan for the treatment of geographic atrophy secondary to age-related macular degeneration (OAKS and DERBY): two multicentre, randomised, double-masked, sham-controlled, phase 3 trials. *Lancet*. 2023;402(10411):1434-1448. doi:10.1016/S0140-6736(23)01520-9

41. Khanani AM, Patel SS, Staurengi G, et al. Efficacy and safety of avacincaptad pegol in patients with geographic atrophy (GATHER2): 12-month results from a randomised, double-masked, phase 3 trial. *Lancet*. 2023;402(10411):1449-1458. doi:10.1016/S0140-6736(23)01583-0
42. Hwang CK, Agrón E, Domalpally A, et al. Progression of Geographic Atrophy with Subsequent Exudative Neovascular Disease in Age-Related Macular Degeneration: AREDS2 Report 24. *Ophthalmol Retina*. 2021;5(2):108-117. doi:10.1016/j.oret.2020.10.008
43. Schmitz-Valckenberg S, Pfau M, Fleckenstein M, et al. Fundus autofluorescence imaging. *Prog Retin Eye Res*. 2021;81:100893. doi:10.1016/j.preteyeres.2020.100893

FIGURES LEGEND.

Figure 1. Multimodal imaging of type 2 macular neovascularization (MNV) in a patient with extensive macular atrophy with pseudodrusen-like appearance (EMAP).

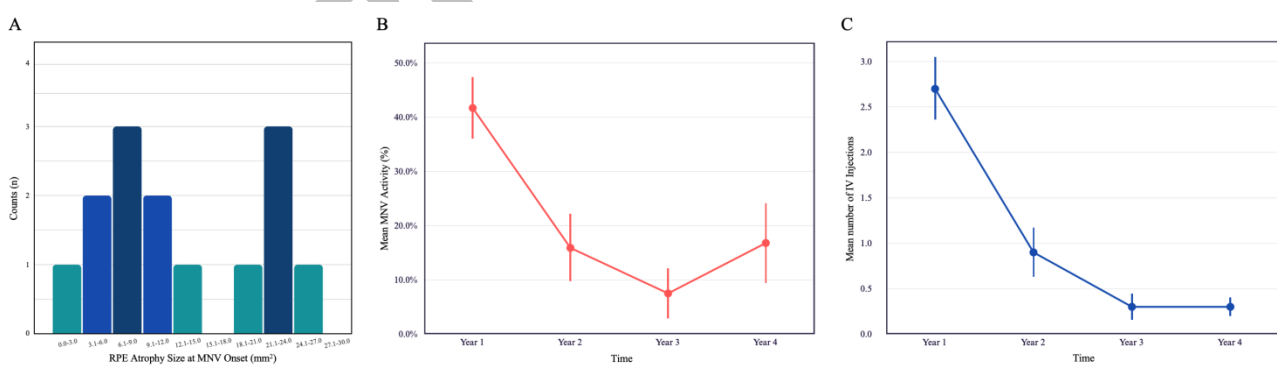


(A) A true-color fundus photograph shows large areas of retinal pigment epithelium (RPE) atrophy with a predominant vertical axis, surrounded by several pseudodrusen-like lesions. A loss of the foveal reflex is visible just inferior to the RPE atrophy. (B) Short-wavelength autofluorescence reveals moderately hypo-autofluorescent areas corresponding to RPE atrophy, with a pronounced hypo-autofluorescent signal superonasal to the fovea.

(C) Early-phase fluorescein angiography displays a hyperfluorescent neovascular membrane, with pronounced leakage in the late phase (E). Indocyanine green angiography highlights the neovascular network (D), with characteristic late-phase staining (F).

Swept-source optical coherence tomography angiography, superimposed on the near-infrared image, provides further visualization of the neovascular network (G). The optical coherence tomography scan through the fovea shows significant neuroretinal thickening due to intraretinal cysts, subretinal hyperreflective material, subretinal neovascularization (H).

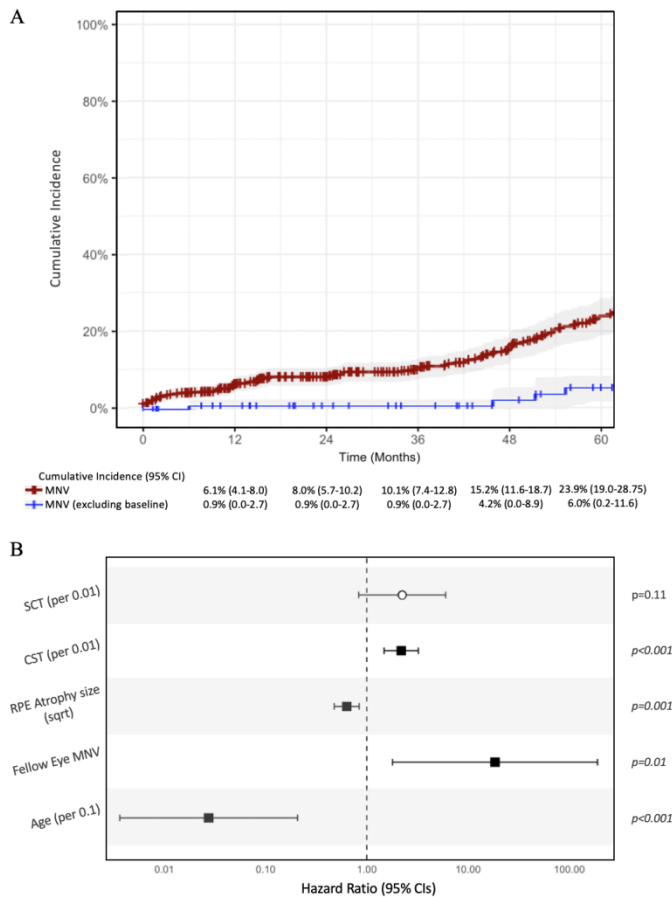
Figure 2. Retinal pigment epithelium (RPE) atrophy size, lesion activity, and intravitreal injection frequency in eyes with extensive macular atrophy with pseudodrusen-like appearance (EMAP) complicated by macular neovascularization (MNV).



(A) A bimodal distribution of MNV development can be observed in relation to RPE atrophy size, with the first peak occurring between 6.1 and 9.0 mm² and the second peak between 21.1 and 24.0 mm². (B) Mean lesion activity was highest in the first year (41.7%) and progressively declined over time, ranging from 7.5 to 16.8% in subsequent years. (C) Similarly, the average number of

intravitreal anti-VEGF injections decreased from 2.7 in the first year to 0.3-0.9 per year during years 2 to 4. Error bars in panels (B) and (C) represent the standard error of the mean.

Figure 3. Cumulative incidence and risk factors for macular neovascularization (MNV) development in extensive macular atrophy with pseudodrusen-like appearance (EMAP).

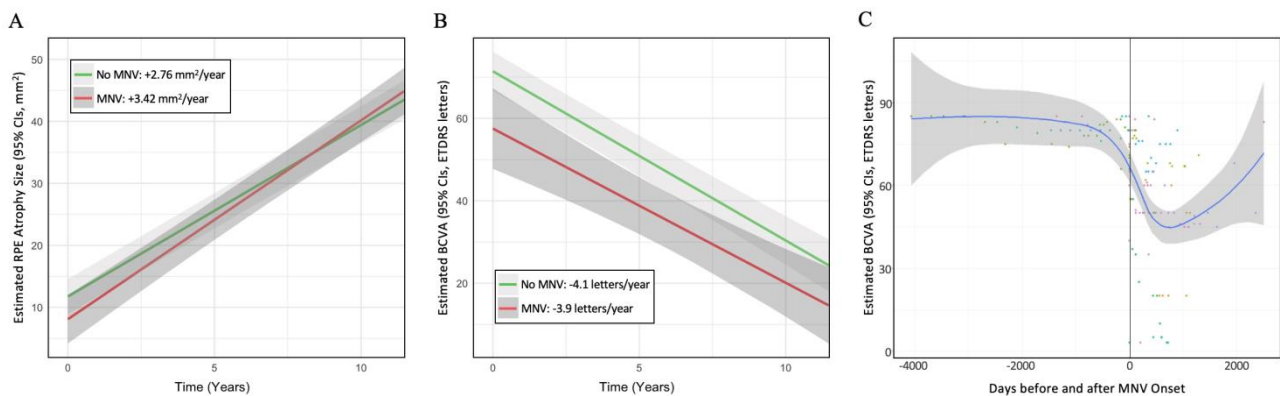


(A) The Kaplan-Meier curve demonstrates a steady increase in MNV cases over time, with a cumulative incidence of 6.1% [95% CI: 4.1-8.0%] at 1 year, rising to 15.2% [95% CI: 11.6-18.7%] by year 4 (red curve). Excluding left-censored data, cumulative incidence was estimated at 0.9% [95% CI: 0.0-2.7] at 1 year and 4.2% [95% CI: 0.0-8.9] at 4 years (blue curve). The 95% confidence intervals are shaded in gray.

(B) Forest plots depict hazard ratios and 95% confidence intervals from a multivariable mixed-effects Cox regression analysis, identifying significant risk factors for MNV development. Notably, greater central subfield thickness (CST; $p<0.001$), smaller retinal pigment epithelium (RPE)

atrophy size ($p=0.001$), fellow eye involvement ($p=0.01$), and younger age ($p<0.001$) were all significantly associated with an increased risk of MNV.

Figure 4. Estimated changes in retinal pigment epithelium (RPE) atrophy size and best-corrected visual acuity (BCVA) between eyes with and without macular neovascularization (MNV) over time.

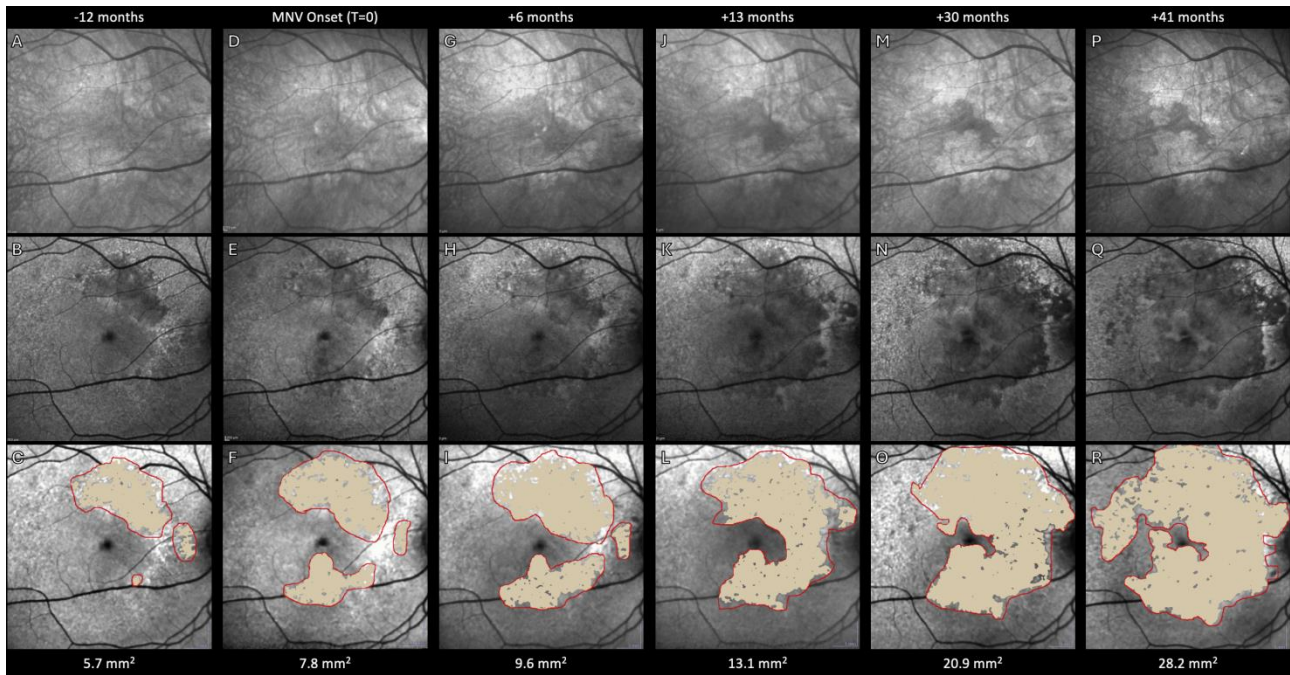


(A) After adjusting for age and baseline areas, eyes with MNV demonstrated a significantly higher rate of RPE atrophy progression compared to eyes without MNV (3.42 vs 2.76 mm^2/year , $p=0.02$).

(B) After adjusting for age and baseline BCVA, no difference in the rate of BCVA decline was observed between eyes with and without MNV (-3.9 vs -4.1 ETDRS letters/year, $p=0.69$).

(C) This panel illustrates the predicted trend of BCVA changes around the onset of MNV, showing a marked decline in BCVA followed by visual improvement after anti-VEGF treatment.

Figure 5. Longitudinal measurement of retinal pigment epithelium (RPE) atrophy in an eye with extensive macular atrophy with pseudodrusen-like appearance (EMAP), complicated by macular neovascularization (MNV), from 12 months before its onset (A-C) to the final follow-up (P-R).



The first row shows near-infrared images used to improve the delineation of RPE atrophy. The second row illustrates the progression of atrophy over time, as captured by short-wavelength autofluorescence (SW-AF). The third row depicts the measured RPE atrophy area using the expert modus of the RegionFinder software (version 2.6.4; Heidelberg Engineering GmbH), with atrophic areas highlighted in yellow and constraints marked in red.

Supplemental Digital Contents

Supplemental Digital Content 1.pdf

Table 1. Demographic and clinical characteristics of the analyzed extensive macular atrophy with pseudodrusen-like appearance (EMAP) cohort.

EMAP Group		
Patients (eyes)	79	(158)
Age years, <i>mean (SD) & median (IQR)</i>	57.2 (5.0)	57.2 (53.8 - 60.5)
Sex		
Males <i>n (%)</i>	27	(34.2%)
Females <i>n (%)</i>	52	(65.8%)
Lens Status		
Phakic eyes <i>n (%)</i>	148	(93.7%)
Pseudophakic eyes <i>n (%)</i>	10	(6.3%)
Smoking Status		
Never <i>n (%)</i>	51	(64.6%)
Former/Current <i>n (%)</i>	5	(6.3%)
Unknown <i>n (%)</i>	23	(29.1%)
Baseline BCVA ETDRS letters, <i>mean (SD) & median (IQR)</i>	70.7 (21.0)	80.0 (65.0 - 84.0)
(Snellen Equivalent)	(20/40)	(20/25)
Baseline RPE Atrophy Size mm ² , <i>mean (SD) & median (IQR)</i>	11.3 (9.0)	8.2 (2.2 - 18.0)
Follow-up months, <i>mean (SD) & median (IQR)</i>	40.4 (34.7)	34.4 (8.3 - 61.3)

Legend: EMAP, extensive macular atrophy with pseudodrusen-like appearance; IQR, interquartile range; BCVA, best-corrected visual acuity; ETDRS, early treatment for diabetic retinopathy study; RPE, retinal pigment epithelium; SD, standard deviation.

Table 2. Clinical and imaging features of extensive macular atrophy with pseudodrusen-like appearance (EMAP) eyes complicated by macular neovascularization (MNV).

EMAP Eyes with MNV		
Eyes (patients)	14 (10)	
MNV Types		
Type 1 <i>n (%)</i>	2 (14.3%)	
Type 2 <i>n (%)</i>	12 (85.7%)	
Type 3 <i>n (%)</i>	0 (0%)	
PCV <i>n (%)</i>	0 (0%)	
MNV Location		
Subfoveal <i>n (%)</i>	9 (64.3%)	
Juxtafoveal <i>n (%)</i>	2 (14.3%)	
Extrafoveal <i>n (%)</i>	3 (21.4%)	
RPE Atrophy Size mm², mean (SD) & median (IQR)	8.5 (9.3)	9.1 (6.2-22.1)
Anti-VEGF Agent used		

Bevacizumab <i>n</i> (%)	7 (50.0%)	
Ranibizumab <i>n</i> (%)	5 (35.7%)	
Aflibercept <i>n</i> (%)	2 (14.3%)	
Time to Fellow Eye Involvement months, <i>mean (SD) & median (IQR)</i>	13.6 (9.2)	11.5 (6.5-17.9)

Legend: EMAP, extensive macular atrophy with pseudodrusen-like appearance; MNV, macular neovascularization; PCV, polypoidal choroidal vasculopathy; RPE, retinal pigment epithelium; IQR, interquartile range; VEGF, vascular endothelial growth factor.

Table 3. Mixed-effects Cox proportional hazards regression analysis assessing the relationship between demographic features, imaging biomarkers, and time-dependent risk of developing macular neovascularization (MNV) in eyes affected by extensive macular atrophy with pseudodrusen-like appearance (EMAP).

Covariates	Cox PH Regression			
	Univariable Analysis		Multivariable Analysis	
	HR (95% CI)	p-value	HR (95% CI)	p-value
Age (0.1)	0.001 (0.0001-0.003)	<0.001	0.03 (0.004-0.21)	<0.001
Smoking Status	2.40 (0.49-11.81)	0.28	-	-
Fellow Eye Involvement	2.14 (1.48-3.07)	<0.001	18.45 (1.79-189.75)	0.01

SW-AF Atrophy Borders	1.39 (0.08-25.51)	0.82	-	-
RPE Atrophy Size (square-rooted)	0.49 (0.45-0.54)	<0.001	0.63 (0.48-0.84)	0.001
VMID	2.39 (0.00-5.79)	0.07	-	-
ORT	0.49 (0.23-1.04)	0.07	-	-
CST (0.01)	2.06 (1.30-3.26)	0.002	2.19 (1.48-3.22)	<0.001
SCT (0.01)	19.06 (7.11-51.08)	<0.001	2.23 (0.83-6.00)	0.11

Legend: PH, proportional hazards; HR, hazard ratio; CI, confidence intervals; SW-AF, short-wavelength autofluorescence; RPE, retinal pigment epithelium; VMID, vitreomacular interface disorder; ORT, outer retinal tubulations; CST, central subfield thickness; SCT, subfoveal choroidal thickness.

Table 4. Clinical and macular neovascularization characteristics in extensive macular atrophy with pseudodrusen-like

	EMAP (our series)	GA	PXE	SFD	L-ORD
--	--------------------------	-----------	------------	------------	--------------

appearance (EMAP) and key phenocopies.

<i>Large Drusen</i>	Absent or rare	Present (sometimes regressed)	Absent	Present from 3rd decade, also nasal to the ONH and along vascular arcades (Sivaprasad S et al. <i>Am J Ophthalmol</i> 2008) (Gliem M et al <i>IOVS</i> 2015)	Absent (Duncan HJ et al. <i>BMJ Open Ophthalmol</i> 2023)
<i>RPD / RPD-like lesions</i>	100%, with pan-retinal distribution (Hamel C et al. <i>Am J Ophthalmol</i>)	>60% (Schmitz-Valckenberg S et al. <i>IOVS</i> 2011)	~50% (age-dependent) (Gliem M et al. <i>JAMA Ophthalmol</i> 2015)	>70% after 6th decade (Gliem M et al <i>Ophthalmology</i> 2015)	100%, from 5th decade (Borooah S et al. <i>Ophthalmol Retina</i> 2021)
<i>BrM Ruptures</i>	25% of late-stage cases (Antropoli et al. <i>Ophthalmology</i> 2024)	16%, especially in the presence of RPD (Sacconi R et al.	85-95% (Finger RP et al. <i>Surv Ophthalmol</i> 2009)	Rare (Capon MR et al. <i>Ophthalmology</i> 1989)	Not documented

		<i>Ophthalmol Ther</i> 2023)			
<i>Choroidal Thickness</i>	Variable at baseline, rapidly thinning (including atrophy) (Romano F et al. <i>Ophthalmol Sci</i> 2021)	Thin (especially in diffuse-trickling SW-AF phenotype) (Lindner M et al. <i>IOVS</i> 2015)	Thinner in the presence of CNV or macular atrophy (Hidalgo-Diaz T et al. <i>Int Ophthalmol</i> 2020)	Thinner with the onset of macular atrophy (Gliem M et al <i>IOVS</i> 2015)	Thin and rapidly thinning (Borooah S et al. <i>Retina</i> 2021)
<i>MNV Frequency</i>	~15% by 4 years	~11% by 4 years (Sunness JS et al. <i>Ophthalmology</i> 1999) (Sacconi R et al. <i>Br J Ophthalmol</i> 2022)	42-86% (Risseeuw S et al. <i>Retina</i> 2019)	60-80% (Sivaprasad S et al. <i>Am J Ophthalmol</i> 2008)	No definitive studies
<i>MNV Types</i>	Type 2 >> type 1; no reports of type 3, PCV, and non-exudative MNV	Type 2 >> type 1 > type 3. Absent/rare PCV. No definitive studies on non-	Type 1 > type 2; no reports of type 3; isolated reports of PCV; non-exudative	Type 2 > type 1 and PCV; no reports of type 3 and non-exudative MNV	No definitive studies: both type 1 and 2 MNV sporadically described (Jeffery

		exudative MNV frequency (Sacconi R et al. <i>Br J Ophthalmol</i> 2022)	MNV (33%) (Cicinelli MV et al. <i>Ophthalmol Retina</i> 2024) (Marques JP et al. <i>Graefes Arch Clin Exp Ophthalmol</i> 2021)	(Sivaprasad S et al. <i>Am J Ophthalmol</i> 2008) (Gliem M et al. <i>IOVS</i> 2015)	RCH et al. <i>Surv Ophthalmol</i> 2024)
MNV Location	Subfoveal >> extrafoveal ≥ juxtafoveal	Subfoveal >> juxta- /extrafoveal (Sacconi R et al. <i>Br J Ophthalmol</i> 2022)	Subfoveal > extrafoveal > juxtafoveal (Rohart C et al. <i>Retina</i> 2023)	Sub-/juxtafoveal > extrafoveal (Sivaprasad S et al. <i>Am J Ophthalmol</i> 2008)	No definitive studies: typically, temporal to the fovea (Jeffery RCH et al. <i>Surv Ophthalmol</i> 2024)
MNV-Atrophy Relationship	Faster progression of atrophy	Slower local progression of atrophy (Pfau M et al. <i>Ophthalmol Retina</i> 2020)	Atrophy associated with type 2 MNV onset and greater extent of AS (Risseuw S et al. <i>Am J Ophthalmol</i>	Unknown; SFD cases without MNV may have faster progression of atrophy	Unknown.

			2020) (Gliem M et al.	
--	--	--	-----------------------	--

			IOVS 2016)	
--	--	--	------------	--

Legend: GA, geographic atrophy; PXE, pseudoxanthoma elasticum; SFD, Sorsby fundus dystrophy; L-ORD, late-onset retinal degeneration; RPD, reticular pseudodrusen; BrM, Bruch's membrane; MNV, macular neovascularization; PCV, polypoidal choroidal vasculopathy; SW-AF, short-wavelength autofluorescence; AS, angioid streaks.